

Depth and Angular Profiles of Inelastic Low-Energy Electron Scattering in Condensed Molecular Samples

Britta Götz,^{†,§} Duška B. Popović,[†] Donald E. David,[†] Josef Michl,^{*,†} and Petra Swiderek[‡]

Department of Chemistry and Biochemistry, University of Colorado, Boulder, Colorado 80309-0215, and
Fachbereich 2, Universität Bremen, Leobener Strasse/NW2, 28334 Bremen, Germany

Received: September 7, 2005; In Final Form: December 19, 2005

Angular distributions of electrons scattered elastically and inelastically from cold solid molecular films of ethylene and nitrogen in various proportions, grown from the gas phase at different temperatures, have been studied by high-resolution electron energy loss spectroscopy. The probing depth of dipole and impact scattering has been investigated by covering the sample by overlayers of argon of increasing thickness. The angular distribution measured for elastically and inelastically dipole-scattered electrons was found to be peaked about the specular direction for all surface conditions studied, while a diffuse angular distribution was possible for electrons that underwent dipole-forbidden scattering. These results allow us to identify favorable conditions for monitoring the composition of a solid sample during the course of reactions occurring under exposure to low-energy electrons.

1. Introduction

Inelastic electron scattering cross sections in solid samples are more difficult to quantify than those in dilute gases. The reason is that in solids not only electron–molecule interactions themselves, that is, dipole, impact, and resonant scattering, but also molecule–solvent interactions, diffraction phenomena,¹ and transport properties of the solid,² and hence its internal structure, contribute to the angular distribution of the scattered electrons. While a reasonable theoretical prediction of gas-phase inelastic electron–molecule scattering by small molecules is now available, for example, propane,^{3,4} a molecule we examined earlier, extension of *ab initio* theory to scattering cross sections of solid samples is still out of reach. An analysis of experimentally determined multiple scattering bands or of the thickness dependence of a specific band yields a qualitative distinction between dipole and impact scattering,⁵ but a highly ordered sample is required to differentiate quantitatively between these contributions to inelastic processes.⁶ Recently, an experimental procedure has been introduced that provides angularly averaged inelastic electron scattering cross sections in molecular solid films by recording the energy distribution of the backscattered electrons as a function of the film thickness.⁷

Reliable inelastic electron scattering cross sections are of interest for determining the composition of solid molecular samples. An example is the measurement of absolute cross sections of electron-induced reactions. Toward this end, recent high-resolution electron energy loss (EEL) spectroscopy experiments have been done to measure the dependence of specific relative inelastic differential scattering cross sections on the level of exposure to electrons with specific energies.^{8–10} The reaction rates have been quantified by mixing the anticipated product into the samples as a standard. This approach raises concern that the measured spectral intensities may not depend linearly

on the quantity of the specific components within a mixture, because, as mentioned above, inelastic differential scattering cross sections may *a priori* depend on the actual structure of the sample. More specifically, one must consider the possibility that the degree of order in the sample, and consequently its diffraction properties, may change during the course of a chemical reaction. As a minimum, this may affect the intensity of dipole scattering processes observed at specific angles. Furthermore, the sample structure may be different when two samples are co-condensed or if one of them is produced in an already existing solid.

In this situation, a careful consideration of the angular distribution of electrons scattered inelastically from molecular films with different structures is required. While the angular distribution for low-energy electrons scattered through long-range dipolar interactions is generally expected to follow essentially the elastic diffraction pattern,¹¹ the situation is more complicated for short-range scattering processes. It has been shown previously that interference between singly and multiply scattered electrons can lead to a pronounced angular variation of the intensity of inelastic short-range (i.e., impact) scattering processes in the case of highly ordered adsorbates.¹² For more disordered molecular multilayer films, one may expect that the electrons that enter the solid will be randomized by multiple scattering processes, most of which will be elastic, before the electrons leave the solid.^{13,14} If this is the case, the angular distribution of inelastically scattered electrons would be diffuse, at least for short-range, dipole-forbidden processes, and a linear dependence of the detected signal intensity on the concentration of a specific compound within a sample would be expected even if the structure of the solid changes. In such a case, standard mixtures could be safely used to quantify the progress of an electron-induced reaction without resorting to a more complicated, explicit determination of angularly averaged inelastic cross sections.⁷

Another problem of relevance to the study of solid molecular films is the probing depth of low-energy electrons. A recent study¹⁵ of the intensity of vibrational excitation bands in EEL

* Corresponding author. E-mail: michl@eefus.colorado.edu.

[†] University of Colorado.

[‡] Universität Bremen.

[§] Current address: Philips Research Laboratories, Prof. Holstlaan 4 (WAG-11), NL 5656 AA Eindhoven, The Netherlands.

spectra as a function of film thickness suggested that long-range dipole scattering probes the film to a depth of several layers while the limited mean free path of electrons within the solid restricts the detection of electrons scattered by short-range interactions to the uppermost layers. While this finding poses another complication to the quantitative comparison of scattering cross sections in solids, it may provide access to the measurement of depth profiles and could help to distinguish between excitations due to dipole and impact scattering.

The aim of the present study is to investigate the angular distribution and the probing depth of low-energy electrons scattered from multilayer, molecular solid films. The study of angular distributions helps to identify conditions that favor diffuse scattering and therefore allows the measurement of reliable reactive scattering cross sections. To this end, EEL spectroscopy has been used to investigate low-energy electron scattering from molecular solid films of different structures, obtained from condensation under different thermodynamically or kinetically controlled conditions or through addition of another compound. The experimental setup used here, described in a previous paper,¹⁶ is particularly well suited for these experiments because it permits molecular films to be prepared at temperatures as low as 4 K. This allows the deposition conditions for films of small molecules to vary over a wide range. Ethylene was chosen as a model compound because its vibrational spectrum is well understood, and therefore the EEL spectra can be easily assigned. Electron scattering from films of pure ethylene and ethylene co-condensed with nitrogen and from ethylene films covered with argon has been investigated. The results of this study answer the question whether impact scattering in molecular multilayer films generally leads to a sufficiently diffuse angular distribution to justify the neglect of any possible anisotropy in the electron scattering when quantifying sample compositions. To obtain information on the probing depth of low-energy electrons scattered from solid samples, EEL spectra have been recorded after covering a molecular film with a rare gas layer of increasing thickness. This simple model system allows us to verify experimentally that the probing depth of dipole scattering is indeed considerably larger than that of impact scattering.

2. Experimental Section

The measurements were performed using a high-resolution LK 2000 EEL spectrometer modified for position-sensitive detection by use of a microchannel plate.¹⁶ The spectrometer is contained in the lowest level of a three-level ion-pumped UHV system capable of maintaining a base pressure of 1×10^{-10} Torr and a minimum pressure of 8×10^{-12} Torr when the cryostat is cooled with liquid He. All samples were deposited from the gas phase onto a Ag(111) crystal substrate mounted at the end of the cryostat, which is rotatable by 360° about the vertical axis of the instrument. The analyzer can be rotated between 80° and 140° with respect to the monochromator, which is fixed. Consequently, a wide range of scattering geometries is accessible, except that a specular geometry can be achieved only for incident angles between 40° and 70° with respect to the surface normal of the sample. The combined resolution of the two energy selectors was between 12 and 20 meV full width at half-maximum (fwhm). The incident energy (E_0) was determined within ± 0.2 eV from the onset of the current transmitted through the deposited films (transmission curve) as measured with a picoammeter. All spectra presented here have been acquired at an incident energy of 2.5 eV, and the energy-loss scale was calibrated to within ± 2 meV by using a second-

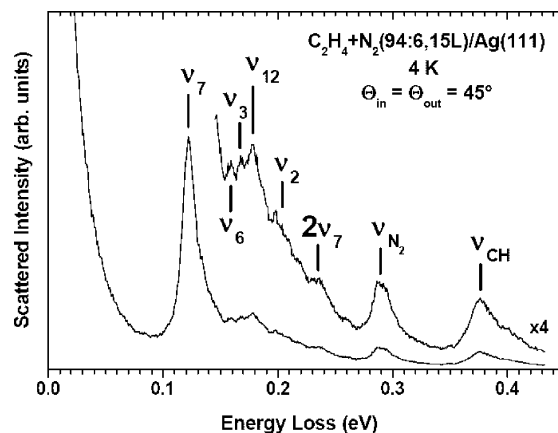


Figure 1. Vibrational EEL spectrum of a 15-layer film produced by co-condensing a mixture of 94% ethylene and 6% N_2 onto Ag(111) at 4 K, recorded under specular conditions ($\theta_{in} = \theta_{out} = 45^\circ$) at an incident energy of 2.5 eV.

order polynomial to relate the arrival position of the electrons on the detector to loss energy as described previously.¹⁶

Ethylene, argon, and nitrogen were purchased from Matheson with stated purities of 99.95%, 99.9995%, and 99% and were used as received. Thin films of these gases were prepared by condensing a gas, or a mixture of gases, onto the Ag(111) crystal, held at a temperature of either 4 or 50 K. The gas mixtures were prepared in a manifold and introduced into the vacuum system via a pulsed valve that was opened for 0.8 ms at a repetition rate of 4 Hz and a diffusor placed directly in front of the crystal. The film thickness was calibrated to an accuracy of $\pm 10\%$ with a quartz microbalance mounted on the sample holder next to the crystal. In all cases, the substrate was cooled to 4 K before acquiring spectra.

Under the deposition conditions used for the formation of overlayers, there is no danger of layer mixing, because the temperature rise of the sample surface is minimal. For instance, when depositing Ar on Ar, the heat load on a 1 cm^2 sample can be estimated as [the latent heat of fusion (29 J/g) + the latent heat of vaporization (161 J/g) + heat capacity (0.5 J/gK) \times temperature change (300 K)] \times mass (1 μg) deposited per time (10 s). This is about 35 μW . The thermal conductivity of solid Ar is 10 mW/cmK, and a sample that is already 50 Å thick will have its temperature raised by about 2 nK, a negligible amount.

3. Results and Discussion

Figure 1 presents a typical EEL spectrum of a multilayer film of ethylene co-condensed with 6% N_2 onto Ag(111) at a temperature of 4 K. The electron incident energy of 2.5 eV used throughout this study was chosen to minimize resonant excitations^{17,18} and to accentuate dipole and impact scattering.

The vibrational mode assignments and loss energies of observed ethylene bands are summarized in Table 1, together with the vibrational energies determined by infrared and Raman experiments. The EEL spectrum (Figure 1) is dominated by the strongly dipole-allowed in-phase, out-of-plane, C–H bending vibration ν_7 , located at 118 meV. Weaker bands in the spectrum correspond to the excitation of vibrations ν_3 (167 meV), ν_6 (159 meV), ν_{12} (179 meV), the C=C stretching mode ν_2 (202 meV), the unresolved C–H stretching modes (377 meV) of ethylene, and the vibration of N_2 (290 meV). In addition, a signal around 233 meV must be due to the first overtone or double excitation of ν_7 . Only the peak intensities of clearly visible features are

TABLE 1: Vibrational Energies of Ethylene (meV)

mode	active	gas ^{24,25}	Ar matrix ²⁶	solid 15 K ²⁵	solid 60 K ²³	solid 79 K ²⁷	present results
ν_{10} (b_{2u})	IR(w)	102.4	103	101.7	101.6 102 102.3		
ν_8 (b_{2g})	Raman	116.5	116.7	117		116.7 117.7	
ν_7 (b_{1u})	IR(vs)	117.7	117.3	116.8 117.9			118
ν_4 (a_u)		126.8		128.4 129.2	128.5 129.2		
ν_6 (b_{1g})	Raman	151.3		152.5		151.5	159
ν_3 (a_g)	Raman	166.4	166.8	166.4 167.5		165 167.1	167
ν_{12} (b_{3u})	IR(s)	179	178.5	178	178.1 178.6		179
ν_2 (a_g)	Raman	201.2	202	200.6		198.6 200.3	202
ν_{11} (b_{3u})	IR(m)	370.6	371.3	368.7			377 (CH)
ν_1 (a_g)	Raman	374.6	375.4	371.8		371.6 372	377 (CH)
ν_5 (b_{1g})	Raman	382.2	383.6	380.6		379.5 380.3	377 (CH)
ν_9 (b_{3u})	IR(s)	385	385.8	383	382.9		377 (CH)

shown in the figures as a function of scattering angle and film thickness.

A. Search for a Diffuse-Scattering Film. Elastic Scattering. The angular distributions of electrons scattered elastically from films of pure ethylene and ethylene co-condensed with nitrogen and argon have been investigated to determine if a sample can be produced that shows diffuse scattering. Figure 2 illustrates how the elastic peak changes when films of pure argon or pure ethylene are grown on the Ag(111) crystal. The width of the elastic peak of electrons scattered from clean Ag(111) is roughly 9° full width at half-maximum (fwhm). This is the expected

angular resolution of the instrument because both the monochromator and the analyzer have transmission angles of 4.6°. The width of the elastic peak increases to 13° fwhm when a film of argon is grown on the Ag(111) surface at 4 K. This slight increase shows that the argon layer must still exhibit a large degree of order. Deposition of ethylene at 50 K widens the elastic peak to about 16° fwhm, implying additional imperfections within the film. Finally, the elastic peak widens to about 20° fwhm for ethylene films grown at 4 K, indicating considerable disorder.¹⁹ This is similar to the results of a LEED study on films of tetracene grown from vapor at low temperatures.²⁰ The LEED pattern in this case did not show distinct spots but diffuse rings at specific angles. This behavior was ascribed to the absence of long-range translational order with characteristic nearest-neighbor distances.²⁰ Correspondingly, in the present case, ethylene is probably only mobile enough immediately after deposition to assume preferred orientations with respect to already deposited neighboring molecules. The resulting short-range order must be sufficient to enhance the specular intensity, that is, zero order diffraction maximum, but must be insufficient to produce really narrow forward scattering.

Figure 3 presents the angular distribution of scattered electrons for several pure and mixed films deposited at 50 or 4 K and measured with an incident angle of either 60° or 65°. Experiments performed on pure ethylene films deposited at both 50 and 4 K essentially reproduce the findings shown in Figure 2, with the widths of the elastic peaks amounting to 18° and 20–34°, respectively, depending upon the exact deposition conditions. Mixing nitrogen with ethylene produces films that show a further increase in the width of the elastic peak and intensity of the diffuse background, giving evidence of additional disorder.

In summary, our results for elastically scattered electrons show that it is not possible, with the deposition rates, temperatures, and gas samples used here, to produce a surface that acts as a true diffuse scatterer. Even if molecules do not diffuse on the surface and a regular lattice cannot be produced due to the presence of different species, evidently, rotational motion during deposition allows the molecules to assume a favorable position with respect to the nearest neighbors. The resulting

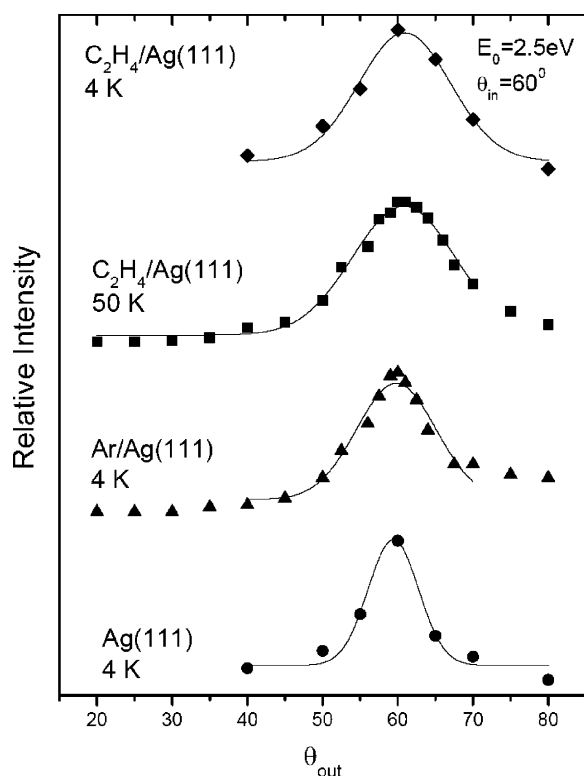


Figure 2. Angular distribution of 2.5 eV electrons scattered elastically from a clean Ag(111) surface and from thin films of argon and ethylene deposited at two temperatures. The angle of incidence was 60°. Film thickness varied between 10 and 15 layers.

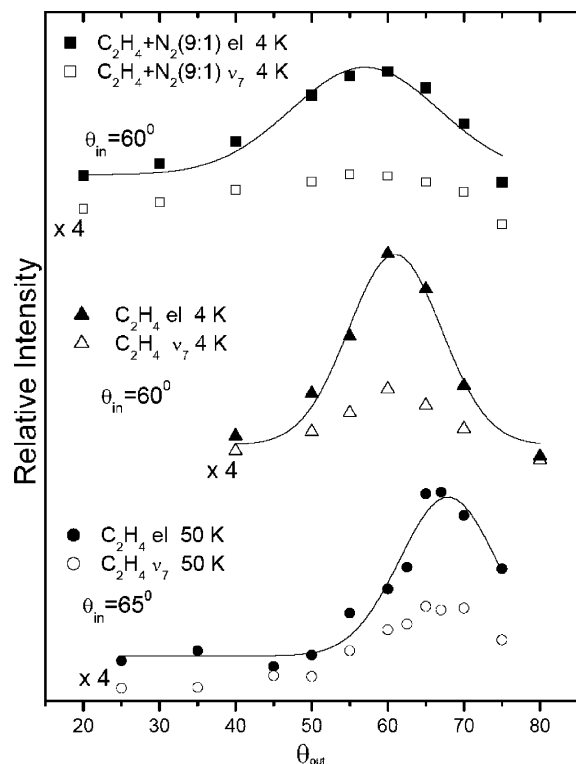


Figure 3. Angular distribution of 2.5 eV electrons scattered elastically (solid symbols) or inelastically upon excitation of ethylene mode ν_7 (open symbols), from films of pure ethylene and ethylene co-condensed with nitrogen and argon deposited on Ag(111) at two temperatures. The film thickness varied between 10 and 15 layers. The incidence angle in the bottom curve is 65° . The data for the elastic band for ethylene at 4 K are the same as those used in Figure 2.

short-range order of the film produces elastic scattering that shows a diffuse background but still peaks around the specular geometry.

Inelastic Scattering. The angular intensity distributions of electrons scattered inelastically by the strongly dipole-allowed ν_7 vibrational mode of ethylene are also shown in Figure 3. The intensity of this mode essentially follows the behavior observed for the elastic peak, demonstrating that a strictly diffuse distribution was not achieved in the case of inelastic dipole scattering.

The angular distributions of the less intense energy loss peaks are shown in Figure 4 for two pure ethylene films. In contrast to elastic scattering and the dipole-allowed mode ν_7 , the angular dependence of intensity for these modes is small. For example, the ν_{12} and the double loss $2\nu_7$ peaks show only slight broad maxima around the specular direction and then only for the film condensed at 50 K. It should be noted that the latter conditions result in the narrowest angular distribution for elastically scattered electrons.

The excitation of the C=C stretching vibration ν_2 does not carry any dipole activity, and C—H stretching excitations have been shown repeatedly to be dominated by impact scattering.^{5,21}

Because Figure 4 shows that these excitations exhibit almost no angular dependence, it may be concluded that impact scattering in solid multilayer molecular films is nearly diffuse, as expected. This is in striking contrast to results obtained previously for ordered adsorbates of CO on a single crystal metal surface, which show a strong variation of impact scattering band intensities with detector angle.¹² This finding was explained by interference between waves scattered directly from a molecule and those that undergo additional elastic scattering processes

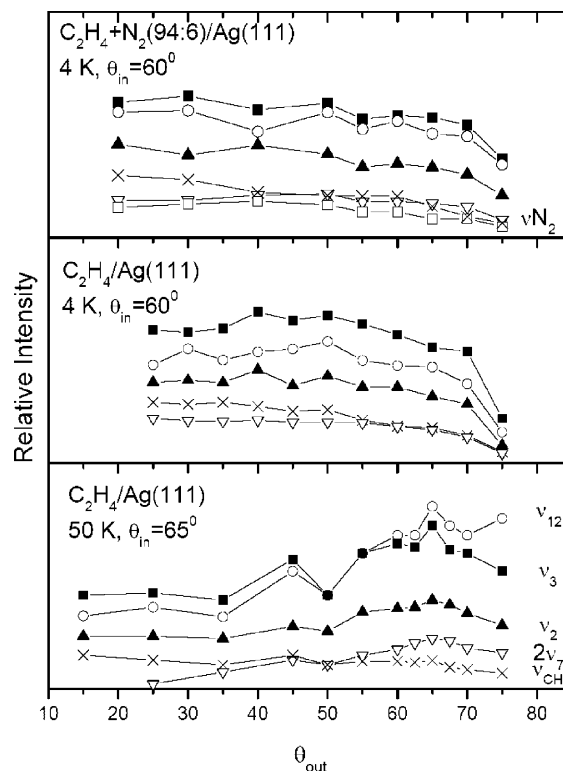


Figure 4. Angular distribution of electrons scattered inelastically from films of pure ethylene and ethylene co-condensed with nitrogen deposited on Ag(111) at two temperatures. The incident energy was 2.5 eV, and the film thickness varied between 10 and 15 layers. The incidence angle in the bottom curve is 65° .

at neighboring atoms.¹² In the present molecular multilayer films, evidently such interference effects are averaged out because of the stochastic nature of the motion of the electrons within the film. Thus, a quantitative approach to electron-induced reaction cross sections that relates the amount of product to the intensities of inelastic losses measured at fixed scattering angles^{8–10} is justified if impact scattering bands are used. Nonetheless, the slight systematic intensity variations observed for impact scattering bands under some conditions (Figure 4) suggested the need for a more thorough investigation. To this end, the intensities of vibrational loss peaks due to impact scattering have been studied as a function of both incident and scattering angle.

Vibrational band intensities vary more strongly as a function of detector angle at small than at large incident angles (Figure 5). This trend may be understood in a straightforward way if one considers the effective path of the electrons within the solid. Electrons that enter the sample at incident angle θ_{in} will travel the distance $l/\cos \theta_{in}$ before scattering inelastically from a molecule located at depth l in the film. Similarly, the distance traveled by the scattered electron moving toward the film–vacuum interface is $l/\cos \theta_{out}$. Thus, the total path traveled in the film is $l(1/\cos \theta_{in} + 1/\cos \theta_{out})$, and the relative intensity of the scattered beam may be expected to vary as

$$\frac{I}{I_0} \propto \frac{1}{1/\cos \theta_{in} + 1/\cos \theta_{out}} \quad (1)$$

The intensity variation expected for this type of dependence is also plotted in Figure 5. The similarity to the observed data is remarkably good considering how many physical effects have been ignored, for example, reflectivity at the vacuum–film and film–substrate interfaces, multiple elastic scattering, and the

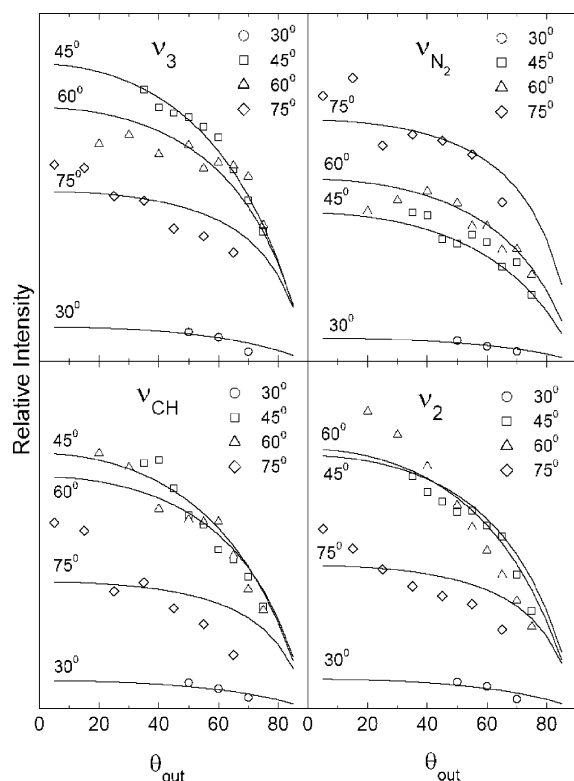


Figure 5. Angular distribution of electrons scattered inelastically from 15-layer films of ethylene co-condensed with nitrogen on Ag(111) at 4 K for different incidence angles and modes of excitation, at incident energy of 2.5 eV. The lines represent eq 1 scaled to the experimental data for each incident angle.

angle dependence of the area illuminated by the electron beam on the sample surface as discussed in detail by Michaud and Sanche.^{13,14} Furthermore, because the energy loss is relatively small, we have assumed that the mean free path of the electrons is the same before and after the inelastic collision. Also, because our films are optically thick, as discussed below, we have ignored the exponential term in eq 6 of ref 13. The predictable angular dependence of our results indicates that a quantitative approach relating the amount of product to the intensities of inelastic losses measured at variable scattering angles is also justified for the case of impact scattering.

In principle, intensity variations could occur for reasons other than changes in detector angle. In the present experiments, several spectra were measured on each film, and it is possible that the electron beam might lead to charging or even to chemical reactions.²² Tests such as repeating the measurements in a different order were performed and have excluded these possibilities.

B. Probing Depth of Electrons and Implications for the Scattering Mechanism. An estimate of the probing depths for vibrational dipole impact scattering, the maximum depths to which an electron can penetrate a film, scatter inelastically, and then escape, can be obtained by measuring the EEL spectra of films of one material successively covered by layers of another material. This was done for films of ethylene covered by 0–101 Å of Ar. The resulting specular and off-specular vibrational EEL spectra are shown in Figure 6.

In accordance with the angular intensity distributions discussed above, the intensities of ν_7 and to some extent also of ν_{12} , both dipole-allowed, are generally smaller at a 30° off-specular than they are at a specular geometry. For a pure ethylene film, ν_3 is less intense than ν_{12} under specular geometry, while the two bands have equal intensities at $\theta_{\text{out}} = 30^\circ$ and

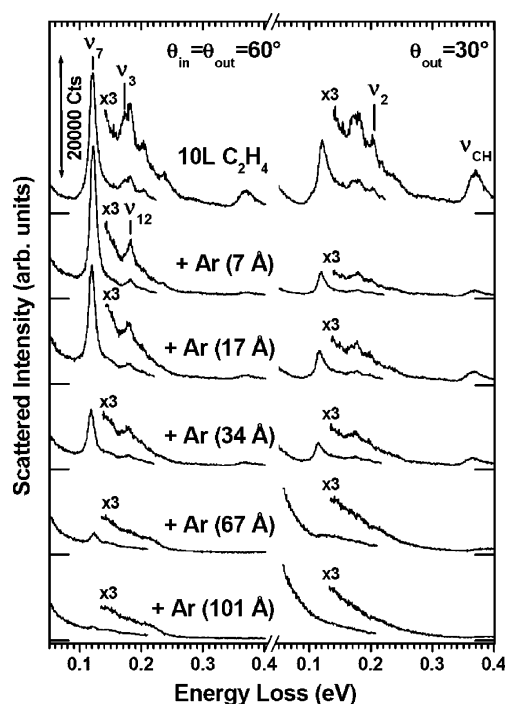


Figure 6. Vibrational EEL spectra of a 10-layer film of ethylene condensed at 4 K, recorded under specular ($\theta_{\text{in}} = \theta_{\text{out}} = 60^\circ$) and off-specular ($\theta_{\text{in}} = 60^\circ$, $\theta_{\text{out}} = 30^\circ$) geometries at an incident energy of 2.5 eV. Also shown are the results for a 10-layer film of ethylene covered by argon at varying thicknesses, measured under the same conditions.

therefore are hard to separate. In contrast, the intensity of the CH stretching band increases when θ_{out} is changed from 60° to 30° due to the larger probing depth at the closer-to-normal detection angle. Because of the smaller probing depth expected for impact scattering, these signals should vanish relatively quickly when a film is covered with a thin overlayer of Ar, while long-range dipole scattering should remain visible at larger thicknesses. Figure 6 shows that this expectation is confirmed. For example, under specular geometry, the intensity of impact band ν_3 drops so rapidly that with an Ar coverage of only 7 Å, the dipole-allowed ν_{12} appears as a single sharp peak. In addition, the differences between the intensities of the dipole-allowed bands ν_7 and ν_{12} under specular versus off-specular geometry increase noticeably upon deposition of two monolayers of Ar, suggesting that the reflectivity of the film increases when it is covered with Ar. This is also evidenced by a narrower angular distribution of the elastic peak (not shown in Figure 6), which increases in intensity by about 50% under specular geometry upon deposition of two monolayers of Ar, yet decreases by 64% at $\theta_{\text{out}} = 30^\circ$. The spectra are dominated by dipole scattering bands at the larger overlayer thickness, although these signals, too, drop successively. At an overlayer thickness of 30 monolayers (101 Å), ν_7 has nearly vanished. This value has also been estimated previously as the upper bound for the interaction range of dipole scattering.²³ On the other hand, impact scattering bands, most noticeably the CH stretching band, remains visible to an Ar thickness of only about 10 monolayers (34 Å).

These results show that dipole and impact scattering can be distinguished easily by their different behavior upon condensation of a very thin overlayer of a different material. The probing depth of dipole scattering through an overlayer of Ar condensed at 4 K is almost 3 times as large as the probing depth for impact scattering under the same conditions. Unfortunately, choosing the optimum thickness for the overlayer is not simple because

the probing depth depends upon the dielectric constant and electron mean free path of the specific material used. Furthermore, the mean free path is a function of both the energy of the incident electron and the structure of the solid, which in turn depends on the deposition temperature. Nonetheless, our findings provide a valuable approach to a facile distinction of dipole and impact scattering excitations in disordered molecular solids.

4. Conclusions

Angle-resolved EEL spectra of solid films of ethylene grown at various temperatures and ethylene co-condensed with nitrogen at 4 K show that diffuse scattering for elastic and inelastic dipole-allowed bands cannot be achieved even when the samples are strongly disordered. The intensities of these bands have maxima in the specular scattering direction in all cases investigated. This behavior is ascribed to persistent short-range order, that is, a preferred orientation of adjacent molecules, even at deposition temperatures as low as 4 K. However, long-range disorder in samples produced at 4 K does broaden the angular distribution and increases the diffuse background. The intensity of specular inelastic dipole scattering actually increases if the overlayer is thin enough and more reflective than the original film.

Impact scattering bands show small intensity variations at different scattering geometries. The angular distribution of these bands is dominated by the path length of electrons within the solid film according to eq 1. In line with the limited probing depth of impact scattering, the intensity of the corresponding bands also decreases more rapidly than that of dipole scattering bands when the film is covered by an overlayer of argon.

The present results suggest that EEL spectroscopic determination of sample composition, for example, detection of changes due to exposure of the sample to an electron beam, should use signals that are not sensitive to changes in the diffraction pattern of the sample with composition. Furthermore, the intensities of these bands should not be limited by the mean free path of the scattered electrons within the sample, which may change with composition. For optically thick films that produce diffuse scattering, eq 1 describes well our observed relative angular distributions. Therefore, we conclude that only impact scattering bands should be used to quantify the relative composition of films. Dipole scattering bands are not good for this purpose because their intensity depends on the order and reflectivity of the sample, both of which may change during the course of reactions that modify the sample. Similarly, a simple comparison of integral scattering cross sections is feasible only for impact scattering bands arising from films that give diffuse scattering.

Acknowledgment. Financial support by the U.S. National Science Foundation (CHE-0446688) and the Deutsche Forschungsgemeinschaft is gratefully acknowledged. B.G. thanks the DAAD for a travel grant.

References and Notes

- (1) Ertl, G.; Küppers, J. *Low Energy Electrons and Surface Chemistry*; VCH: Weinheim, 1985.
- (2) Michaud, M.; Lepage, M.; Sanche, L. *Phys. Rev. B* **1999**, *59*, 15480.
- (3) Popović, D. B.; David, D. E.; Michl, J.; Čurik, R.; Čársky, P. *J. Chem. Phys.* **2004**, *121*, 10551.
- (4) Polášek, M.; Juřek, M.; Ingr, M.; Čársky, P.; Horáček, J. *Phys. Rev. A* **2000**, *61*, 032701.
- (5) Götz, B.; Winterling, H.; Swiderek, P. *J. Electron Spectrosc.* **1999**, *105*, 1.
- (6) Magnée, R.; Mekhalif, Z.; Doneux, C.; Duwez, A.-S.; Gregoire, C.; Riga, J.; Delhalle, J.; Pireaux, J. J. *J. Electron Spectrosc.* **1998**, *88–91*, 855.
- (7) Lévesque, P. L.; Michaud, M.; Sanche, L. *J. Chem. Phys.* **2005**, *122*, 094701.
- (8) Lepage, M.; Michaud, M.; Sanche, L. *J. Chem. Phys.* **1997**, *107*, 3478.
- (9) Lepage, M.; Michaud, M.; Sanche, L. *J. Chem. Phys.* **2000**, *113*, 3602.
- (10) Swiderek, P.; Deschamps, M. C.; Michaud, M.; Sanche, L. *J. Phys. Chem. B* **2004**, *108*, 11850.
- (11) Persson, B. N. *Solid State Commun.* **1977**, *24*, 573.
- (12) Tong, S. Y.; Li, C. H.; Mills, D. L. *Phys. Rev. B* **1981**, *24*, 806.
- (13) Michaud, M.; Sanche, L. *Phys. Rev. B* **1984**, *30*, 6067.
- (14) Sanche, L.; Michaud, M. *Phys. Rev. B* **1984**, *30*, 6078.
- (15) Götz, B.; Kröhl, O.; Swiderek, P. *J. Electron Spectrosc.* **2001**, *114–116*, 569.
- (16) David, D. E.; Popović, D. B.; Antic, D.; Michl, J. *J. Chem. Phys.* **2004**, *121*, 10542.
- (17) Okuyama, H.; Kato, H.; Kawai, M.; Yoshinobu, J. *J. Chem. Phys.* **2000**, *113*, 2866.
- (18) Walker, I. C.; Stamatović, A.; Wong, S. F. *J. Chem. Phys.* **1978**, *69*, 5532.
- (19) Woodruff, D. P.; Delchar, T. A. *Modern Techniques of Surface Science*; Cambridge University Press: New York, 1986.
- (20) Eiermann, R.; Parkinson, G. M.; Bäessler, H.; Thomas, J. M. *J. Phys. Chem.* **1983**, *87*, 544.
- (21) Winterling, H.; Haberkern, H.; Swiderek, P. *Phys. Chem. Chem. Phys.* **2001**, *3*, 4592.
- (22) Ibach, H.; Mills, D. L. *Electron Energy Loss Spectroscopy and Surface Vibrations*; Academic Press: New York, 1982.
- (23) Sanche, L. *Phys. Rev. Lett.* **1995**, *75*, 2904.
- (24) Duncan, J. L.; McKean, D. C.; Mallinson, P. D. *J. Mol. Spectrosc.* **1973**, *45*, 221.
- (25) Duncan, J. L.; Hegelund, F.; Foster, R. B.; Hills, G. W.; Jones, W. *J. Mol. Spectrosc.* **1976**, *61*, 470.
- (26) Cowieson, D. R.; Barnes, A. J.; Orville-Thomas, W. J. *J. Raman Spectrosc.* **1981**, *10*, 224.
- (27) Blumenfeld, S. M.; Paddi Reddy, S.; Welsh, H. L. *Can. J. Phys.* **1970**, *48*, 513.